06

Specific effects of high-energy gas plasma flows on the properties of the piezoelectric ceramics

© G.Yu. Sotnikova,[1] G.A. Gavrilov,[1] N.V. Zaitseva,[1] R.S. Passet,[1,2] A.V. Sotnikov[2]

[1]Ioffe Institute,
194021 St. Petersburg, Russia
[2]Emperor Alexander I St. Petersburg State Transport University,
190031 St. Petersburg, Russia
e-mail: gga_holo@mail.ru

Received July 11, 2025
Revised July 30, 2025
Accepted August 10, 2025

The study of the influence of repeated high-energy ($0.4\,\mathrm{MJ/m^2}$) gas plasma flows on the main material parameters of the industrial piezoelectric CTSNV-1 and CTS-19 ceramics is presented. The preservation of the crystalline structure and polarization of the samples under repeated extreme thermal load plasma exposure is experimentally confirmed. A small decrease in the main material parameters of the ceramic samples is observed during the first 10 pulses of the exposure, as well as their subsequent return and stabilization at the near-initial levels with a further increase in the number of pulses up to 80. It is assumed that this effect is associated with the observed modification of the surface layer microstructure of the ceramic, which stabilizes by the $10-20$ th pulse of exposure regardless of the plasma-forming gas composition.

Keywords: piezoelectric ceramics, gas plasma, surface modification, extreme thermal loads, material parameters.

DOI: 10.61011/TP.2026.02.62884.177-25

Introduction

Piezoelectric ceramics are classified as functional materials having a unique set of electrophysical properties, with the piezoelectric effect being the key one. Thoroughly elaborated and cost effective piezoelectric ceramics manufacturing technology has laid the basis for their wide use as a base material for ultrasonic transducers, sensors of various physical quantities, precision actuators and piezoelectric motors [1]. Solid solution systems based on lead zirconate-titanate (PZT), $Pb(Ti_{1-x}Zr_x)O_3$, are the basis of a considerable part of modern piezoelectric ceramics. Such materials have exceptional piezoelectric and electromechanical properties, composition and microstructure variability, which was reflected in a wide range of domestically-made industrial ceramics. Review [2] states the relevant areas for improvement of piezoceramic materials synthesis techniques, where increased stability of piezoelectric component performance with a necessary set of constitutive constants to environmental impacts plays the core role. This is primarily related to an increase in the operating temperature limit of piezoelectric ceramics defined by the Curie temperatures, T_C, at which phase transition takes place, leading to disappearance of electric polarization and, consequently, loss of essential functionality. PZT piezoelectric ceramics feature relatively low $T_C = 190\,^\circ\mathrm{C} - 400\,^\circ\mathrm{C}$ depending on its composition, thus significantly limiting the operating range of use, which is generally within $0.5-0.8\,T_C$ [2]. Successful solution of this problem imposes a requirement for the development of experimental techniques for investigating the resistance of piezoelectric ceramics properties to high-energy external loads, in particular, to the impact of plasma fluxes with various compositions, densities and particle energies. The latter is related to the prospect of using piezoelectric ceramics as a material for actuators in International Thermonuclear Experimental Reactor (ITER) diagnostics systems developed by the Ioffe Institute [3]. One of the key problems with using piezoelectric materials in thermonuclear facilities is the radiation resistance of these materials [4–6]. Theoretical analysis of radiation effect on PZT ceramics properties was performed in [4]. It was shown that with the expected level of radiation effect these compounds basically have a good potential resistance to amorphization and depolarization due to radiation. However, inadequate focus is made on maintaining the performance of piezoelectric materials under the action of uncontrolled high-energy plasma loads, in particular, random plasma ejections occurring at the edges of plasma (edge localized mode, ELM events) [7]. Note that regardless of the progress in the area of lead-free piezoelectric materials development, lead-containing piezoelectric ceramics is still widely used for creating a range of electromechanical devices capable of working in extreme conditions, including radiation (see [5,6] and references therein).

Study [8] has first experimentally proved that CTSNV-1 ceramics samples maintain their structure, polarization and piezoelectric response when exposed to 20 hydrogen plasma pulses with flux energies of $0.03\ \mathrm{MJ/m^2}$ and $0.2\,\mathrm{MJ/m^2}$ (thermal load power is about $1\ \mathrm{GW/m^2}$ and $7\ \mathrm{GW/m^2}$, predicted surface temperatures of samples are $\geq 400\,^\circ\mathrm{C}$ and $\geq 1000\,^\circ\mathrm{C}$, respectively), which potentially suggests that

plasma techniques may be used for creating thermal barrier coatings on the PZT ceramics surface and can be considered as one of promising research areas in the framework of modern concepts of microstructural design of piezoceramic materials [9].

Change of surface layer structure and properties due to plasma-induced defects is known to be used in various processes, including creating thermal barrier coatings [10] without changing bulk properties of materials. High-energy monokinetic ion flows with various intensities are used to form localized „defect layers“ at the desired depth in materials, which is the basis of dislocation-free silicon-on-insulator technologies. Such structures are widely used in microelectronic components with high radiation and thermal resistance [11]. Incident ion scattering and implantation, particle emission from a material exposed to ion bombardment, and change of near-surface layer structure and properties due to plasma-induced defects are being widely studied [12,13 and references therein]. Despite long-term investigations, phenomena observed when the surface of materials is exposed to plasma cannot be unambiguously explained within the existing theoretical models even for metals, which are more simple objects compared with piezoelectric ceramics [14]. Thus, studies of structural changes and related properties of ferroelectric and piezoelectric materials are of key importance for fundamental understanding of processes induced in them by external extreme impacts and for the development of techniques for creating functional components with high radiation and thermal resistance.

To explain physical phenomena induced by high energy pulsed plasma flow and to find possible mechanisms preventing degradation of bulk properties of piezoelectric ceramics, obtaining reproducible and reliable experimental data as well as dependable data interpretation are required.

The aim of this work is to demonstrate an experimental technique for dosed exposure to helium and hydrogen plasma fluxes with the desired energy level, and to provide the quantitative estimates of their influence on the properties of PZT-based industrial piezoceramics.

1. Experiment

1.1. Selecting research objects

A key factor for elaboration of the initial experimental technique is the ability to produce a sufficient quantity of samples with stable batch-to-batch parameters using a well-proven mass production technology.

Samples of commercially available mass-produced CTS-19 and CTSNV-1 („Avrora–Elma“, Volgograd, Russia) ceramics were chosen as test objects. By the concentration of main components, these compounds fall within the morphotropic phase boundary region (MPB) [15]: Zr/Ti = 58/42 for CTSNV-1 and Zr/Ti = 53/47 for CTS-19. It is known that two different ferroelectric phases: tetragonal (T-phase) and rhombohedral (Rh-phase), can co-exist in the MPB region, and the highest piezoelectric activity of the material is observed [15]. By the set of piezoelectric constant parameters ($d_{33} = 300$ pC/N for CTS-19 and $d_{33} = 425$ pC/N for CTSNV-1), relative permittivity ($\varepsilon_{33} = 1600$ for CTS-19 and $\varepsilon_{33} = 2325$ for CTSNV-1), and relatively high Curie temperatures ($T_C = 290\,^\circ$C for CTS-19 and $T_C = 240\,^\circ$C for CTSNV-1) [2], CTS-19 and CTSNV-1 are classified among the best domestic piezomaterials designed for a wide range of applications.

Ceramic samples of both types consisted of discs 10 mm in diameter and 1 mm in thickness with baked Ag electrodes. Polarization of samples was performed by the manufacturer in accordance with the manufacturer's specifications. One sample of each type was left as a virgin sample while the rest were exposed to hydrogen and helium plasma with various degree of intensity. Before exposure, electrodes were removed from surfaces of all samples. Samples were irradiated through the electrodeless surface along the polarization direction. For measurement of electrophysical parameters of samples after irradiation, electrodes were applied to the exposed surfaces using highly dispersed silver paste and dried for 24 hours at room temperature.

1.2. Experimental procedure

Experiments used a pulsed plasma facility provided by the Ioffe Institute (plasma gun bench) designed for investigating the interaction between plasma and protective materials of the ITER first wall exposed to significant thermal loads [16]. Jet source is a coaxial plasma accelerator with intense feed of test gas, which defines the isotopic composition of plasma. It provides formation of pulsed (duration $\sim 20\,\mu$s) dense flux of particles ~ 45 mm in diameter with an energy of 100−300 eV, moving at a velocity up to 100 km/s. Flux energy density determined by the capacitive storage voltage and the distance to the sample can reach 1 MJ/m^2. Note that the most informative parameter for pulsed plasma thermal loads is the heat flux factor F_{HF}, [MW/(m$^2\cdot$ s$^{1/2}$)] because it considers the duration and, consequently, the depth of heat wave penetration into a material at the initial stage of thermal diffusion processes typical of short-term energy impact.

In several series of experiments, samples were placed at different distances (300 mm, 370 mm and 900 mm) from the plasma accelerator outlet, which provided different sample exposure energy densities in accordance with the flux parameters described in [16]: 0.2 MJ/m^2, 0.1 MJ/m^2 and 0.03 MJ/m^2. This corresponds to design thermal loads on a sample, F_{HF}: 40 MW, 20 MW and 6 MW/(m$^2\cdot$ s$^{1/2}$). The expected rapid increase of surface temperature is about 2000 °C, 1500 °C and 500 °C respectively. For analysis of piezoelectric ceramics resistance to such thermal loads, samples were exposed to various numbers of plasma pulses, which is reflected on their marking: „test gas“ – „number of exposure pulses“, for example, He-30 and H2-30 mean that

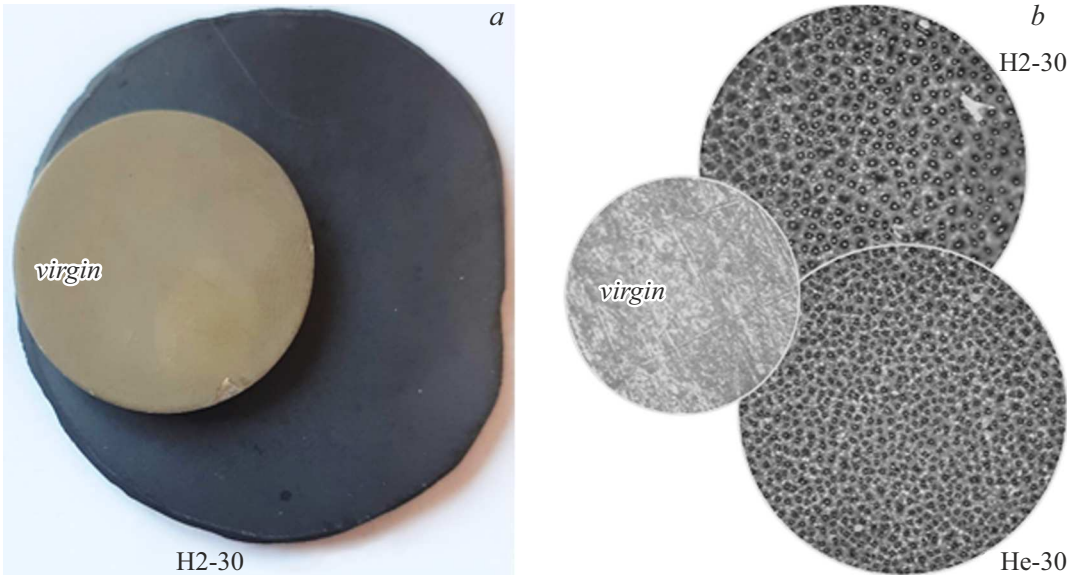

Figure 1. Optical (a) and SEM images (b) of virgin and exposed CTSNV-1 ceramic samples surfaces: samples H2-30 and He-30 were obtained through exposure to 30 hydrogen and helium plasma pulses with the same jet parameters (particle energy ~ 100 eV, duration $\sim 20\,\mu$s, $F_{HF} \approx 20\,\text{MW}/(\text{m}^2 \cdot \text{s}^{1/2})$).

ceramics samples were exposed to 30 helium and hydrogen plasma pulses.

1.3. Modification of surface layer structure and composition

Structural changes of sample surfaces were studied using the X-ray diffraction analysis, optical and scanning electron microscopy (SEM) techniques. Initial visual examination has shown gradual darkening of surface, which by exposure pulse 20−30 acquires a typical black color (Figure 1, a) for both types of ceramics regardless of the isotopic composition of plasma. Figure 1, b shows photographs of surface areas of CTSNV-1 samples, both virgin and exposed to 30 hydrogen and helium plasma pulses at $F_{HF} = 20\,\text{MW}/(\text{m}^2 \cdot \text{s}^{1/2})$, made using the Nikon Eclipse LV100 microscope. It can be clearly seen that the surfaces of exposed samples undergo significant modification, attaining a pronounced relief with typical nonuniformity sizes of the order of $20\,\mu$m depending on the plasma composition. Helium plasma forms a finer nonuniformity structure than hydrogen plasma. However, for hydrogen plasma, typical microstructure is formed as early as by exposure pulse 20 without undergoing significant quality changes as the number of pulses further increases. For helium plasma, microstructure formation is completed in the interval between pulse 10 and pulse 30, and also has no visible quality changes as the number of pulses further increases.

Phase structure of the surface was examined using the Dron-3 X-ray diffractometer (CuK_α radiation). Analysis of diffraction patterns of both piezoelectric ceramics compositions after exposure to He and H2 plasma fluxes until 100 exposure pulses at $F_{HF} = 20\,\text{MW}/(\text{m}^2 \cdot \text{s}^{1/2})$ has shown that the samples generally retained their single-phase structure and had no amorphization signs. At the same time, diffraction patterns of the exposed samples show reflections not belonging to the ferroelectric phase structure typical of both compounds of interest.

For purposes of illustration, Figure 2 shows diffraction patterns of various CTSNV-1 piezoelectric ceramics surface segments with an area about $5\,\text{mm}^2$ for virgin sample and samples H2-20 exposed to hydrogen plasma with different flux energies.

Flux energy was varied from 0.2 MJ/m^2 to 0.03 MJ/m^2 by placing the samples at distances 300 mm and 900 mm from the plasma accelerator outlet, which corresponds to heat loads on a sample $F_{HF}(300\,\text{mm}) = 40\,\text{MW}/(\text{m}^2 \cdot \text{s}^{1/2})$ and $F_{HF}(900\,\text{mm}) = 6\,\text{MW}/(\text{m}^2 \cdot \text{s}^{1/2})$. The same figure shows a line diagram of CTSNV-1 corresponding to a known molar concentration ratio Zr/Ti = 58/42. The figure shows reflections not belonging to the initial sample structure.

Black color of the surface of exposed samples and pronounced reflections in the area of 27−30 degrees on the diffraction pattern of a sample exposed to high energy impact (Figure 2, d) were qualified earlier in [8] as lead dioxide structures, α-PbO_2, in the form of black rhombic crystals (line diagram in Figure 2, e).

Further electron microscopy analysis of the surface elemental composition has shown that the observed structural changes have a more complex nature.

Figure 3 shows SEM images of the CTSNV-1 sample surface area, to which diffraction pattern in Figure 2, d corresponds.

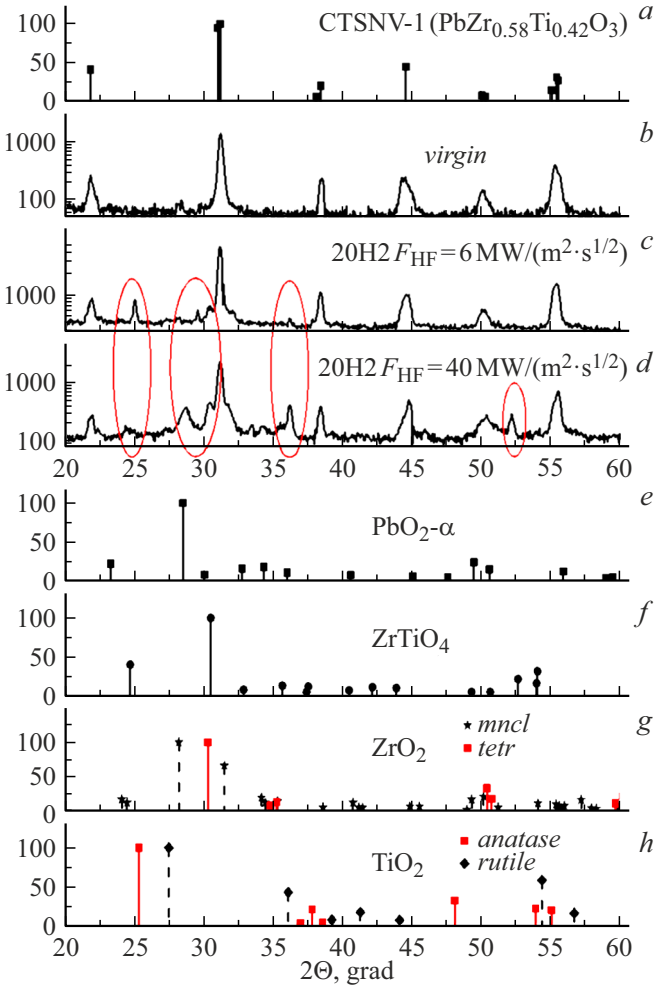

Figure 2. Bar diagram of PZT compound close to CTSNV-1 by the concentration of main components (a), diffraction patterns of samples before (b) and after (c,d) exposure to 20 hydrogen plasma exposure with various heat flux powers, bar diagrams of expected new crystalline structures formed on the surface of samples as a result of plasma impact (e–f).

There is a pronounced relief in the form of „hills“ with round top and typical diameters and heights of about 10–20 μm. Elemental analysis of surface has shown essentially inhomogeneous distribution of main chemical elements of ceramics: a region between the „hills“ approximately corresponds to the initial composition, while the surface of „hills“ has a leadless crystalline structure corresponding to the ZrO_2–TiO_2 solid solution structure (see colored inset in Figure 3), various modifications of which depend on the thermodynamic conditions of synthesis. Detailed analysis of phase transformations and equilibrium phase states for PZT ceramics, being a quaternary O–Pb–Ti–Zr system, is described, for example, in [17], where PbO–ZrO_2–TiO_2 and ZrO_2–TiO_2 phase diagrams are shown in a wide temperature range from 300 °C to 3000 °C. In particular, it is reported that $Zr_xTi_{1-x}O_4$ solid solutions with Zr:Ti molar ratio from 1:1 to 1:2 are the only stable compounds in the ZrO_2–TiO_2 system at high synthesis temperatures. They undergo gradual transition to the ordered state in the temperature range between 1400 K and 1100 K, which agrees with the expected surface temperatures of samples at $F_{HF} = 40\,\mathrm{MW/(m^2 \cdot s^{1/2})}$. At temperatures above 1400 K, $ZrTiO_4$ crystallizes in the α-PbO type orthorhombic structure with random distribution of Zr and Ti. Bar diagrams of possible modifications of ZrO_2–TiO_2 are shown in Figure 2, e–h.

For more detailed analysis of PZT ceramics for high energy plasma load resistance, a series of samples was prepared and tested. The samples were exposed to various numbers (10, 30, 70, 100) of He and H2 plasma pulses at a constant flux energy level of 0.1 MJ/m^2 by placing the samples at a distance of 370 mm from the plasma accelerator outlet, which corresponds to $F_{HF} = 20\,\mathrm{MW/(m^2 \cdot s^{1/2})}$.

Diffraction spectra of virgin samples of both types of ceramics are identical and close to the tetragonal ferroelectric phase structure, which is most typical of the test samples. Detailed analysis of diffraction patterns of both types of ceramics has shown a qualitatively identical pattern of structural changes in samples as the number of exposure pulses of both He and H2 plasma increased. As an example, Figure 4 shows a series of diffraction patterns of CTS-19 samples before and after exposure to plasma, and bar diagrams of the initial and expected surface layer structures (ZrO_2–TiO_2). It can be seen that as early as at the first 10 exposure pulses, there are noticeable changes in the diffraction spectra, which are more clearly pronounced in case of H2 plasma exposure.

The observed transformation of reflections (101) and (002)–(200) suggests that there is possible morphotropic transformation between two ferroelectric phases of the initial composition [14].

Additional reflections occurring at (101) confirms that a ZrO_2–TiO_2 structure has formed, and peaks occurring within $2\Theta = 25 - 30°$ illustrate superlattice reflections of $ZrTiO_4$, whose positions and intensity depend on the rate of cooling below the synthesis temperature of about 1200 °C [18].

It is obvious that the observed structural modification of sample surfaces after plasma exposure shall affect the change of their physical characteristics.

1.4. Measurements of the main constitutive parameters of PZT ceramic samples

The following constitutive parameters were taken as plasma load resistance acceptance criteria for piezoelectric ceramics: relative permittivity ε_{33}, dielectric loss tangent $\tan(\delta)$, speed of sound, piezoelectric constants (e_{33} and d_{33}) and electromechanical coupling coefficient of thickness oscillation mode k_t. Preliminary parameter measurements were performed on virgin samples of polarized CTSNV-1 and CTS-19 ceramics from the same batch. The measured data generally appeared to be close to the manufacturer's data [www.avrora-elma.ru]. Measurements and calculations

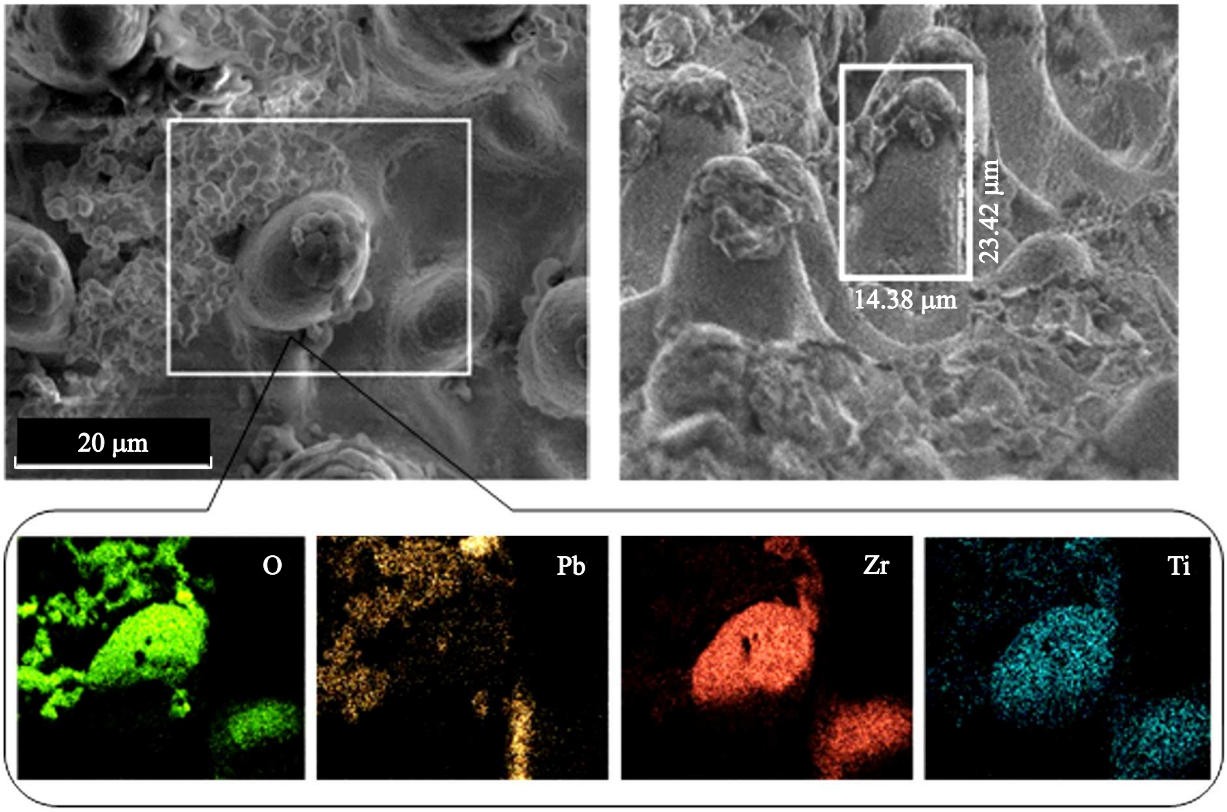

Figure 3. Magnified SEM images of the CTSNV-1 sample surface exposed to 20 hydrogen plasma pulses with $F_{HF} = 40\,\mathrm{MW/(m^2 \cdot s^{1/2})}$. Inset — distribution of main elements in the selected region of the formed „hill-like" microstructure.

were performed in accordance with recommendations of IEEE Standards ANSI/IEEE 176−1987.

ε_{33} and $\tan(\delta)$ were measured using the impedance meter. V_L (longitudinal mode) was measured using a standard pulse-echo technique, acoustic wave excitation and reception were performed using the Kropus ultrasound transducers. Independent measurements of V_L along the polarization and ε_{33} directions determine the piezoelectric constant e_{33} [19].

Electromechanical coupling coefficient of thickness oscillation mode k_t was determined from experimentally measured electromechanical resonance frequencies of thickness-mode piesoelectric resonators using the frequency ratio of series (f_s) and parallel (f_p) resonances of the fundamental resonance mode [20].

Study [21] describes in detail all measurement techniques and provides measurements of both types of ceramics (CTS-19 and CTSNV-1) exposed to up to 30 plasma jet pulses with $F_{HF} = 20\,\mathrm{MW/(m^2 \cdot s^{1/2})}$. Experiments have shown qualitatively similar (with some quantitative differences) dependences of dielectric and piezoelectric constants on the number of exposure pulses for both H2 and He plasmas and both ceramics compositions. For both types of piezoelectric ceramics, He plasma exerts stronger influence on dielectric and piezoelectric properties than H2 plasma. An unusual behavior of parameters was observed i.e. minor, but noticeable deviation from values typical of virgin samples after the first several exposure pulses, followed by restoration of initial values as the number of exposure pulses further increased. Since the measurements for CTS-19 ceramics in [21] were limited by 30 plasma pulses, experimental measurements of the main constitutive parameters of ceramics with an increase in the degree of plasma exposure to 100 pulses with the same intensity along and opposite to the polarization direction are of obvious interest. Figure 5 shows the measurements and calculations of the main constitutive parameters of CTS-19 ceramics after repeated exposure to He and H2 plasmas for particle flux directions along (solid symbols) and opposite (empty symbols) to the polarization direction of virgin samples.

Data in Figure 5, supplementing the previous results [21], are indicative of a stable polarization preservation effect under repeated pulsed high energy plasma loads with up to 70 pulses. However, at pulse 100 there is noticeable decrease in e_{33} and k_t with preservation of the main dielectric parameters and speed of sound. Exposure direction (along or opposite to the initial polarization of material) has no influence on the qualitative behavior of observed changes and introduces just insignificant quantitative deviations.

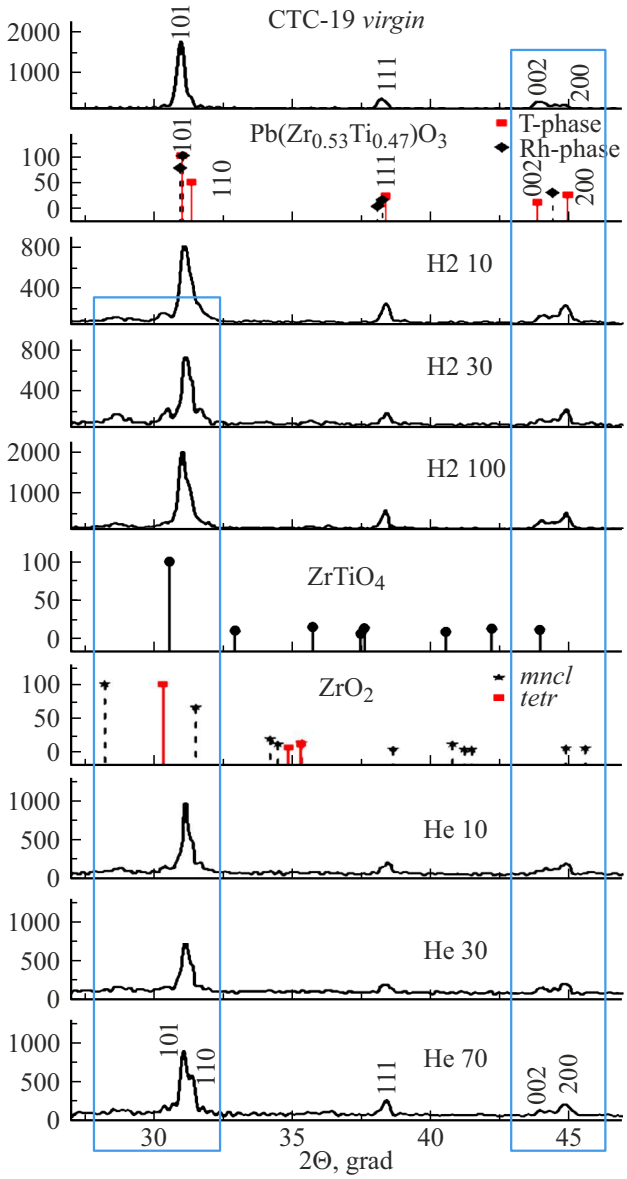

Figure 4. Bar diagrams of initial composition CTS-19 and expected surface layer structure (ZrO_2–$ZrTiO_4$). Diffraction patterns of samples before and after exposure to hydrogen and helium plasma pulses with $F_{HF} = 20\,\mathrm{MW/(m^2 \cdot s^{1/2})}$.

2. Discussion of findings

Analysis of the experimental findings shows that unusual behavior of PZT-based piezoceramic materials (Figure 4) is directly associated with formation of modified near-surface layer, which reaches some steady state as the number of plasma exposure pulses increases. Typical surface relief sizes and observed changes in phase and elemental compositions of near-surface layer are defined by the level of thermal load per plasma jet exposure pulse. The magnitude of thermal load defines the temperature behavior of the PZT piezoelectric ceramics sample, launching the surface layer melting/amorphization/recrystallization processes and forming a new space structure on the basis of ZrO_2–TiO_2.

The most interesting is the experimentally established stabilization of piezoelectric properties of samples exposed to sufficiently long series of high energy pulses regardless of a minor degradation of properties at the initial exposure stage. Significant decrease in piezoelectric properties and electromechanical coupling coefficient occurs only at exposure pulse 100.

We believe that this is caused by the fact that changes in the material structure, phase composition and, consequently, polarization occur exclusively within the near-surface layer, whose steady-state depth (at plasma exposure pulse 20–30) is not larger than several tens of micrometers, which is maximum 10 % of the initial sample thickness. Modified layer depth will expectedly grow as the number of plasma pulses increases and will be followed by further decrease in material polarization. The observed significant decrease in piezo- and electromechanical constants with the increase in the number of pulses to 100 can indicate that there are some „threshold“ plasma exposure doses which is the subject of further experimental studies.

X-ray diffraction analysis, optical and electron microscopy data shown in Section 2.3 are indicative of partial formation of a new structure on the basis of ZrO_2–TiO_2 compounds, various modifications and phase state of which depend on thermodynamic conditions of synthesis under the action of high energy plasma flux. In particular, study [22] demonstrates the synthesis of $ZrTiO_4$ ceramics with a grain size of 10 – 30 nm during heating of such system to a temperature above 1200 °C followed by fast cooling. It is also known that grain boundaries serve as natural sinks for point defects [23]. Thus, as can be expected, structures with typical grain sizes in the area of tens of nanometers and, consequently, with high boundary density will have high radiation resistance. Moreover, such structure on the ceramics surface will additionally play a role of thermal barrier due to exclusive thermophysical properties of zirconium titanate [22].

At the initial plasma exposure stage (before 10 pulses), surface layer modification is accompanied by inhomogeneous decrease in its polarization due to heating above the Curie temperature, leading to insignificant degradation of piezoelectric properties of samples. Further restoration and preservation of piezoelectric properties with increase in the number of exposure pulses (at least up to 70) can be attributed to full depolarization of near-surface layer when it doesn't influence the piezoelectric bulk properties of the sample any longer. The result is that the electromechanical coupling coefficient is restored in all cases. The observed PZT ceramics surface microstructuring effects caused by plasma fluxes with various ion compositions cannot be fully explained and described within the existing theoretical models [24–26] and references therein]. Studies [25,26] develop a theory of electrocapillary instability of metal surface based on charge redistribution on metal surface under the action of electric field generated in the laser

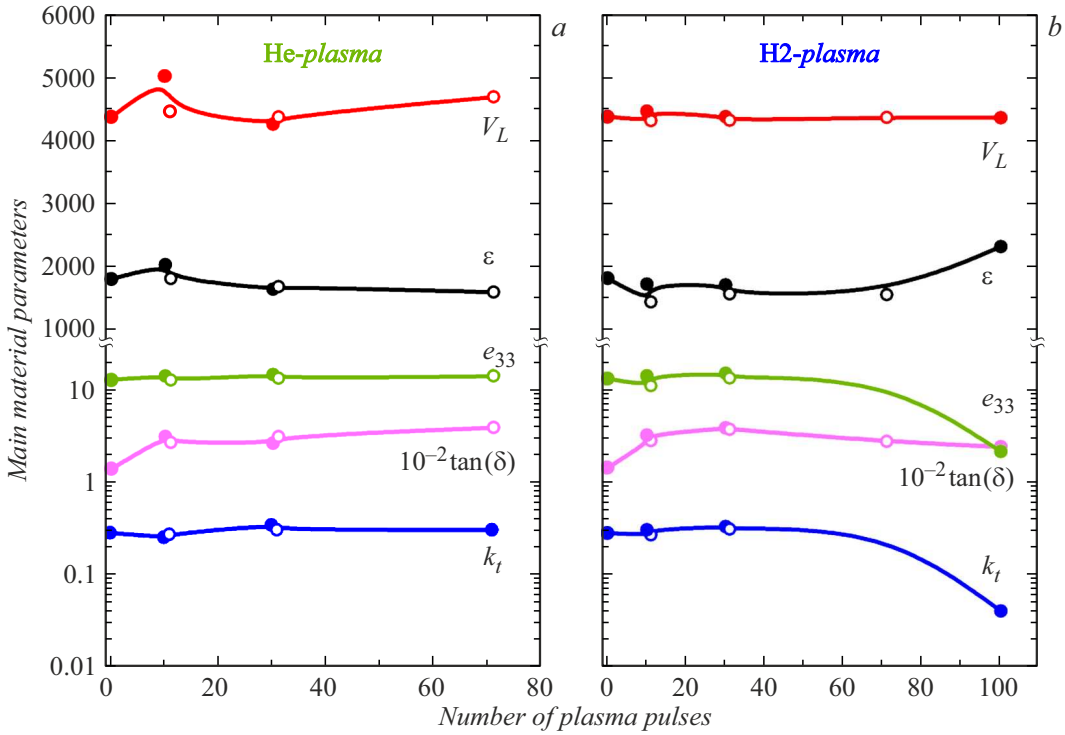

Figure 5. Main constitutive parameters of CTS-19 ceramics depending on the number of pulses of helium (a) and hydrogen (b) plasma jets with $F_{HF} = 20\,\mathrm{MW/(m^2 \cdot s^{1/2})}$. Solid symbols on the curves correspond to plasma jet impact along the initial sample polarization direction, empty symbols correspond to plasma jet impact opposite to the initial sample polarization direction.

flare plasma. This leads to a change in interaction forces between molecules on the surface, which is displayed as a change in surface tension, and can lead to various forms of deformation, including formation of waves, protrusions and even surface discontinuities. However, electrophysical properties of metals differ considerably from those of ferroelectric materials (dielectric materials), and laser flare plasma provides the passage of significant current, which considerably distinguishes it from electrically neutral gas plasma fluxes described in this work. Akhmanov et al. [24] have proposed a thermal model for describing various physical phenomena occurring in surface layers of solid bodies (metals, semiconductors and dielectric materials) under the action of high power laser heat pulses. It is shown that thermodynamic instability conditions implemented via fast (tens of nanoseconds) heating of the lattice followed by fast melting of the surface layer lead to spatially inhomogeneous surface heating and, consequently, can lead to observed changes in phase and elemental compositions in the near-surface layer of PZT piezoelectric ceramics and to formation of new ordered structures on it. It appears that quasiperiodic structures on the surface of piezoelectric ceramics samples exposed to gas plasma pulses (Figure 1, b) can be described within a thermal model [24], which adequately agrees with the thermal mechanism of nanocrystalline structure formation. $ZrTiO_4$ [22].

Conclusion

Comprehensive experimental study of the dynamics of both surface structure and a of set of dielectric, piezoelectric and electromechanical parameters of industrial samples of CTS-19 and CTSNV-1 piezoelectric ceramics under the action of high energy helium and hydrogen plasma fluxes is presented.

Experimental demonstration of preserved polarization in all samples regardless of repeated extremely high energy pulsed loads is the main result of the study.

Dependences of dielectric, piezoelectric and electromechanical parameters on the number of plasma exposure pulses characterized by a thermal factor of $20\,\mathrm{MW/(m^2 \cdot s^{1/2})}$ were obtained for both types of piezoelectric ceramics. Some decrease in parameters was observed after the first 5–10 exposure pulses. Further increase in the number of pulses led to stabilization of the main material parameters for both types of ceramics to the values typical of unexposed samples. The observed „restoration“ effect correlates with formation of a specific „hill-like“ surface microstructure with changed elemental composition and typical sizes of several tens of micrometers. However, after 70 pulses of extremely high thermal exposure, there is a noticeable reduction of piezoelectric activity due to gradual depolarization of bulk samples.

Possible surface layer modification mechanisms leading to recrystallization of the surface layer with modification of

the elemental composition, and related effects of change, restoration and preservation of the main constitutive parameters of piezoelectric ceramics are discussed. In addition, even the first experimental results obtained for industrial piezoelectric ceramics show that a barrier layer can be formed on the surface of PZT materials, preventing the devastating effect of high energy pulsed impact loads on the main constitutive parameters. This stimulates further study of mechanisms of plasma influence on the properties of ferroelectric and piezoelectric materials, including the investigation of maximum permissible energy properties of plasma impact.

Acknowledgments

The authors are grateful to V.Yu. Goryainov (Ioffe Institute) for preparation of samples and A.V. Nashchekin (Ioffe Institute) for electron microscopy examinations performed on the equipment provided by the Federal Joint Research Center „Material science and characterization in advanced technology".

Funding

The work was partially supported by grant of the Russian Science Foundation № 24-19-00716 (https://rscf.ru/project/24-19-00716/).

Conflict of interest

The authors declare no conflict of interest.

References

[1] K. Uchino (editor). *Advanced piezoelectric materials, Second Edition* (Woodhead Publishing in Materials, 2017), DOI: 10.1016/B978-0-08-102135-4.00001-1

[2] A.E. Panich. Phys. Bases Instrument., **8** (1 (31)), 30 (2019). DOI: 10.25210/jfop-1901-030035

[3] E.E. Mukhin, V.M. Nelyubov, V.A. Yukish, E.P. Smirnova, V.A. Solovei, N.K. Kalinina, V.G. Nagaitsev, M.F. Valishin, A.R. Belozerova, S.A. Enin, A.A. Borisov, N.A. Deryabina, V.I. Khripunov, D.V. Portnov, N.A. Babinov, D.V. Dokhtarenko, I.A. Khodunov, V.N. Klimov, A.G. Razdobarin, S.E. Alexandrov, D.I. Elets, A.N. Bazhenov, I.M. Bukreev, An.P. Chernakov, A.M. Dmitriev, Y.G. Ibragimova, A.N. Koval, G.S. Kurskiev, A.E. Litvinov, K.O. Nikolaenko, D.S. Samsonov, V.A. Senichenkov, R.S. Smirnov, S.Yu. Tolstyakov, I.B. Tereschenko, L.A. Varshavchik, N.S. Zhiltsov, A.N. Mokeev, P.V. Chernakov, P. Andrew, M. Kempenaars. Fusion Engineering and Design, **176**, 113017 (2022). DOI: 10.1016/j.fusengdes.2022.113017

[4] E.E. Mukhin, E.P. Smirnova, N.A. Babinov, I.A. Khodunov, R.S. Smirnov, M.S. Kuligin. Tech. Phys. Lett., **48** (12), 4 (2022). DOI: 10.21883/TPL.2022.12.54935.19208

[5] D.A. Parks, B.R. Tittmann. IEEE Transactions on Ultrasonics, Ferroelectrics, and Frequency Control, **61** (7), 1216 (2014). DOI: 10.1109/TUFFC.2014.3020

[6] E.P. Smirnova, V.N. Klimov, E.G. Guk, P.A. Pankratiev, N.V. Zaitseva, A.V. Sotnikov, E.E. Mukhin. Phys. Solid State, **65** (11), 1888 (2023). DOI: 10.61011/PSS.2023.11.57323.206

[7] A.V. Voronin, V.K. Gusev, Ya.A. Gerasimenko, E.V. Demina, I.V. Miroshnikov, E.E. Mukhin, A.N. Novokhatsky, Yu.V. Petrov, M.D. Prusakova, N.V. Sakharov, P.B. Shchogolev. Plasma Phys. EPS Conf. **1**, 601 (2013).

[8] G.Yu. Sotnikova, A.V. Voronin, V.Yu. Goryainov, N.V. Zaytseva, V.N. Klimov, A.V. Nashekin, R.S. Passet, A.V. Sotnikov. Tech. Phys. Lett., **50** (2), 21 (2024). DOI: 10.61011/PJTF.2024.03.57040.19735

[9] A.N. Rybianets. *Porous ceramics and piezocomposites: modeling, technology, and characterization*. In A.Newton (editor). *Advanced in porous ceramics*, Chapter 2 (Nova Science Publishers Inc., NY., 2017)

[10] N. Markocsan, M. Gupta, S. Joshi, P. Nylén, X.-H. Li, J. Wigren. J. Therm. Spray. Tech., **26**, 1104 (2017). DOI: 10.1007/s11666-017-0555-4

[11] J. Hunn, E. Lee, T. Byun, L. Mansur. J. Nucl. Mater., **282**, 131 (2000). DOI: 10.1016/0022-3115(95)00054-2

[12] P. Hatton, D. Perez, T. Frolov, B.P. Uberuaga. Acta Mater., **269**, 119821 (2024). DOI: 10.1016/j.actamat.2024.119821

[13] C. Stancu, V. Marascu, A. Bonciu, A. Bercea, S.D. Stoica, C. Constantin. Materials, **16** (21), 6853 (2023). DOI: 10.3390/ma16216853

[14] F. Sanchez, L. Marot, A. Dmitryev, R. Steiner, E. Meyer. Fusion Engineering and Design, **200**, 114187 (2024). DOI: 10.1016/j.fusengdes.2024.114187

[15] V.A. Isupov. Phys. Solid State, **43** (12), 2262 (2001). DOI: 10.1134/1.1427954

[16] A.V. Voronin, V.K. Gusev, Y.A. Gersimenko, Y.V. Sud'enkov. Tech. Phys., **58** (8), 1122 (2013). DOI: 10.1134/S1063784213080264.

[17] M. Cancarevic, M. Zinkevich, F. Aldinger. J. Ceramic Society Jpn., **114** (11), 937 (2006). DOI: 10.2109/jcersj.114.937

[18] Y. Park, Y. Kim. Mater. Res. Bull., **31** (1), 7 (1996). DOI: 10.1016/0025-5408(95)00172-7

[19] S.V. Bogdanov. Acoust. Phys., **46** (5), 530 (2000). DOI: 10.1134/1.1310376

[20] S. Sherrit, B.K. Mukherjee, arXiv. 0711.2657 (2007). DOI: 10.48550/arXiv.0711.2657

[21] G.Yu. Sotnikova, A.V. Ankudinov, A.V. Voronin, G.A. Gavrilov, A.L. Glazov, V.Yu. Goryainov, N.V. Zaitseva, A.V. Nashchekin, R.S. Passet, A.A. Vorob'ev, A.V. Sotnikov. Ceramics, **7** (4), 1695 (2024). DOI: 10.3390/ceramics7040108

[22] A.K. Bachina, O.V. Almjasheva, D.P. Danilovich, V.I. Popkov. Russ. J. Phys. Chem., **95** (8), 1529 (2021). DOI: 10.1134/S0036024421080057

[23] X.M. Bai, B.P. Uberuaga. JOM, **65**, 360 (2013). DOI: 10.1007/s11837-012-0544-5

[24] S.A. Akhmanov, V.I. Emel'yanov, N.I. Koroteev, V.N. Seminogov. Sov. Phys. Usp., **28**, 1084 (1985). DOI: 10.1070/PU1985v028n12ABEH003986

[25] A.A. Bormatov, V.M. Kozhevin, S.A. Gurevich. Tech. Phys., **66** (5), 705 (2021). DOI: 10.1134/S1063784221050078

[26] V.M. Kozhevin, M.V. Gorokhov, A.A. Bormatov. Tech. Phys. Lett., **43** (7), 670 (2017). DOI: 10.1134/S1063785017070203

Translated by E.Ilyinskaya